DESY-09-077

DESY–09–077
June 9, 2009

arXiv:0906.1424v1 [hep-ex] 8 Jun 2009

# Measurement of $J/\psi$ helicity distributions in inelastic photoproduction at HERA

ZEUS Collaboration

**Abstract**

The $J/\psi$ decay angular distributions have been measured in inelastic photoproduction in $ep$ collisions with the ZEUS detector at HERA, using an integrated luminosity of 468 pb$^{-1}$. The range in photon-proton centre-of-mass energy, $W$, was $50 < W < 180$ GeV. The $J/\psi$ mesons were identified through their decay into muon pairs. The polar and azimuthal angles of the $\mu^+$ were measured in the $J/\psi$ rest frame and compared to theoretical predictions at leading and next-to-leading order in QCD.

# The ZEUS Collaboration

S. Chekanov, M. Derrick, S. Magill, B. Musgrave, D. Nicholass[1], J. Repond, R. Yoshida
*Argonne National Laboratory, Argonne, Illinois 60439-4815, USA* [n]

M.C.K. Mattingly
*Andrews University, Berrien Springs, Michigan 49104-0380, USA*

P. Antonioli, G. Bari, L. Bellagamba, D. Boscherini, A. Bruni, G. Bruni, F. Cindolo, M. Corradi, G. Iacobucci, A. Margotti, R. Nania, A. Polini
*INFN Bologna, Bologna, Italy* [e]

S. Antonelli, M. Basile, M. Bindi, L. Cifarelli, A. Contin, S. De Pasquale[2], G. Sartorelli, A. Zichichi
*University and INFN Bologna, Bologna, Italy* [e]

D. Bartsch, I. Brock, H. Hartmann, E. Hilger, H.-P. Jakob, M. Jüngst, A.E. Nuncio-Quiroz, E. Paul, U. Samson, V. Schönberg, R. Shehzadi, M. Wlasenko
*Physikalisches Institut der Universität Bonn, Bonn, Germany* [b]

J.D. Morris[3]
*H.H. Wills Physics Laboratory, University of Bristol, Bristol, United Kingdom* [m]

M. Kaur, P. Kaur[4], I. Singh[4]
*Panjab University, Department of Physics, Chandigarh, India*

M. Capua, S. Fazio, A. Mastroberardino, M. Schioppa, G. Susinno, E. Tassi
*Calabria University, Physics Department and INFN, Cosenza, Italy* [e]

J.Y. Kim
*Chonnam National University, Kwangju, South Korea*

Z.A. Ibrahim, F. Mohamad Idris, B. Kamaluddin, W.A.T. Wan Abdullah
*Jabatan Fizik, Universiti Malaya, 50603 Kuala Lumpur, Malaysia* [r]

Y. Ning, Z. Ren, F. Sciulli
*Nevis Laboratories, Columbia University, Irvington on Hudson, New York 10027, USA* [o]

J. Chwastowski, A. Eskreys, J. Figiel, A. Galas, K. Olkiewicz, B. Pawlik, P. Stopa, L. Zawiejski
*The Henryk Niewodniczanski Institute of Nuclear Physics, Polish Academy of Sciences, Cracow, Poland* [i]

L. Adamczyk, T. Bołd, I. Grabowska-Bołd, D. Kisielewska, J. Łukasik[5], M. Przybycień, L. Suszycki
*Faculty of Physics and Applied Computer Science, AGH-University of Science and Technology, Cracow, Poland* [p]

A. Kotański[6], W. Słomiński[7]
*Department of Physics, Jagellonian University, Cracow, Poland*

O. Behnke, J. Behr, U. Behrens, C. Blohm, K. Borras, D. Bot, R. Ciesielski, N. Coppola, S. Fang, A. Geiser, P. Göttlicher[8], J. Grebenyuk, I. Gregor, T. Haas, W. Hain, A. Hüttmann, F. Januschek, B. Kahle, I.I. Katkov[9], U. Klein[10], U. Kötz, H. Kowalski, M. Lisovyi, E. Lobodzinska, B. Löhr, R. Mankel[11], I.-A. Melzer-Pellmann, S. Miglioranzi[12], A. Montanari, T. Namsoo, D. Notz, A. Parenti, P. Roloff, I. Rubinsky, U. Schneekloth, A. Spiridonov[13], D. Szuba[14], J. Szuba[15], T. Theedt, J. Tomaszewska[16], G. Wolf, K. Wrona, A.G. Yagües-Molina, C. Youngman, W. Zeuner[11]
*Deutsches Elektronen-Synchrotron DESY, Hamburg, Germany*

V. Drugakov, W. Lohmann, S. Schlenstedt
*Deutsches Elektronen-Synchrotron DESY, Zeuthen, Germany*

G. Barbagli, E. Gallo
*INFN Florence, Florence, Italy* [e]

P. G. Pelfer
*University and INFN Florence, Florence, Italy* [e]

A. Bamberger, D. Dobur, F. Karstens, N.N. Vlasov[17]
*Fakultät für Physik der Universität Freiburg i.Br., Freiburg i.Br., Germany* [b]

P.J. Bussey, A.T. Doyle, M. Forrest, D.H. Saxon, I.O. Skillicorn
*Department of Physics and Astronomy, University of Glasgow, Glasgow, United Kingdom* [m]

I. Gialas[18], K. Papageorgiu
*Department of Engineering in Management and Finance, Univ. of the Aegean, Chios, Greece*

U. Holm, R. Klanner, E. Lohrmann, H. Perrey, P. Schleper, T. Schörner-Sadenius, J. Sztuk, H. Stadie, M. Turcato
*Hamburg University, Institute of Exp. Physics, Hamburg, Germany* [b]

K.R. Long, A.D. Tapper
*Imperial College London, High Energy Nuclear Physics Group, London, United Kingdom* [m]

T. Matsumoto, K. Nagano, K. Tokushuku[19], S. Yamada, Y. Yamazaki[20]
*Institute of Particle and Nuclear Studies, KEK, Tsukuba, Japan* [f]

A.N. Barakbaev, E.G. Boos, N.S. Pokrovskiy, B.O. Zhautykov
*Institute of Physics and Technology of Ministry of Education and Science of Kazakhstan, Almaty, Kazakhstan*

V. Aushev[21], O. Bachynska, M. Borodin, I. Kadenko, O. Kuprash, V. Libov, D. Lontkovskyi, I. Makarenko, Iu. Sorokin, A. Verbytskyi, O. Volynets, M. Zolko
*Institute for Nuclear Research, National Academy of Sciences, and Kiev National University, Kiev, Ukraine*

D. Son
*Kyungpook National University, Center for High Energy Physics, Daegu, South Korea* [g]

J. de Favereau, K. Piotrzkowski
*Institut de Physique Nucléaire, Université Catholique de Louvain, Louvain-la-Neuve, Belgium* [q]

F. Barreiro, C. Glasman, M. Jimenez, J. del Peso, E. Ron, J. Terrón, C. Uribe-Estrada
*Departamento de Física Teórica, Universidad Autónoma de Madrid, Madrid, Spain* [l]

F. Corriveau, J. Schwartz, C. Zhou
*Department of Physics, McGill University, Montréal, Québec, Canada H3A 2T8* [a]

T. Tsurugai
*Meiji Gakuin University, Faculty of General Education, Yokohama, Japan* [f]

A. Antonov, B.A. Dolgoshein, D. Gladkov, V. Sosnovtsev, A. Stifutkin, S. Suchkov
*Moscow Engineering Physics Institute, Moscow, Russia* [j]

R.K. Dementiev, P.F. Ermolov †, L.K. Gladilin, Yu.A. Golubkov, L.A. Khein, I.A. Korzhavina, V.A. Kuzmin, B.B. Levchenko[22], O.Yu. Lukina, A.S. Proskuryakov, L.M. Shcheglova, D.S. Zotkin
*Moscow State University, Institute of Nuclear Physics, Moscow, Russia* [k]

I. Abt, A. Caldwell, D. Kollar, B. Reisert, W.B. Schmidke
*Max-Planck-Institut für Physik, München, Germany*

G. Grigorescu, A. Keramidas, E. Koffeman, P. Kooijman, A. Pellegrino, H. Tiecke, M. Vázquez[12], L. Wiggers
*NIKHEF and University of Amsterdam, Amsterdam, Netherlands* [h]

N. Brümmer, B. Bylsma, L.S. Durkin, A. Lee, T.Y. Ling
*Physics Department, Ohio State University, Columbus, Ohio 43210, USA* [n]

A.M. Cooper-Sarkar, R.C.E. Devenish, J. Ferrando, B. Foster, C. Gwenlan[23], K. Horton[24], K. Oliver, A. Robertson, R. Walczak
*Department of Physics, University of Oxford, Oxford United Kingdom* [m]

A. Bertolin, F. Dal Corso, S. Dusini, A. Longhin, L. Stanco
*INFN Padova, Padova, Italy* [e]

R. Brugnera, R. Carlin, A. Garfagnini, S. Limentani
*Dipartimento di Fisica dell' Università and INFN, Padova, Italy* [e]

B.Y. Oh, A. Raval, J.J. Whitmore[25]
*Department of Physics, Pennsylvania State University, University Park, Pennsylvania 16802, USA* [o]

Y. Iga
*Polytechnic University, Sagamihara, Japan* [f]

G. D'Agostini, G. Marini, A. Nigro
*Dipartimento di Fisica, Università 'La Sapienza' and INFN, Rome, Italy* [e]

J.C. Hart
*Rutherford Appleton Laboratory, Chilton, Didcot, Oxon, United Kingdom* [m]

H. Abramowicz[26], R. Ingbir, S. Kananov, A. Levy, A. Stern
*Raymond and Beverly Sackler Faculty of Exact Sciences, School of Physics, Tel Aviv University,*
*Tel Aviv, Israel* [d]

M. Ishitsuka, T. Kanno, M. Kuze, J. Maeda
*Department of Physics, Tokyo Institute of Technology, Tokyo, Japan* [f]

R. Hori, S. Kagawa[27], N. Okazaki, S. Shimizu, T. Tawara
*Department of Physics, University of Tokyo, Tokyo, Japan* [f]

R. Hamatsu, H. Kaji[28], S. Kitamura[29], O. Ota[30], Y.D. Ri
*Tokyo Metropolitan University, Department of Physics, Tokyo, Japan* [f]

M. Costa, M.I. Ferrero, V. Monaco, R. Sacchi, V. Sola, A. Solano
*Università di Torino and INFN, Torino, Italy* [e]

M. Arneodo, M. Ruspa
*Università del Piemonte Orientale, Novara, and INFN, Torino, Italy* [e]

S. Fourletov[31], J.F. Martin, T.P. Stewart
*Department of Physics, University of Toronto, Toronto, Ontario, Canada M5S 1A7* [a]

S.K. Boutle[18], J.M. Butterworth, T.W. Jones, J.H. Loizides, M. Wing[32]
*Physics and Astronomy Department, University College London, London, United Kingdom* [m]

B. Brzozowska, J. Ciborowski[33], G. Grzelak, P. Kulinski, P. Łużniak[34], J. Malka[34], R.J. Nowak, J.M. Pawlak, W. Perlanski[34], A.F. Żarnecki
*Warsaw University, Institute of Experimental Physics, Warsaw, Poland*

M. Adamus, P. Plucinski[35]
*Institute for Nuclear Studies, Warsaw, Poland*

Y. Eisenberg, D. Hochman, U. Karshon
*Department of Particle Physics, Weizmann Institute, Rehovot, Israel* [c]

E. Brownson, D.D. Reeder, A.A. Savin, W.H. Smith, H. Wolfe
*Department of Physics, University of Wisconsin, Madison, Wisconsin 53706*, USA [n]

S. Bhadra, C.D. Catterall, G. Hartner, U. Noor, J. Whyte
*Department of Physics, York University, Ontario, Canada M3J 1P3* [a]

[1] also affiliated with University College London, United Kingdom
[2] now at University of Salerno, Italy
[3] now at Queen Mary University of London, United Kingdom
[4] also working at Max Planck Institute, Munich, Germany
[5] now at Institute of Aviation, Warsaw, Poland
[6] supported by the research grant No. 1 P03B 04529 (2005-2008)
[7] This work was supported in part by the Marie Curie Actions Transfer of Knowledge project COCOS (contract MTKD-CT-2004-517186)
[8] now at DESY group FEB, Hamburg, Germany
[9] also at Moscow State University, Russia
[10] now at University of Liverpool, United Kingdom
[11] on leave of absence at CERN, Geneva, Switzerland
[12] now at CERN, Geneva, Switzerland
[13] also at Institut of Theoretical and Experimental Physics, Moscow, Russia
[14] also at INP, Cracow, Poland
[15] also at FPACS, AGH-UST, Cracow, Poland
[16] partially supported by Warsaw University, Poland
[17] partially supported by Moscow State University, Russia
[18] also affiliated with DESY, Germany
[19] also at University of Tokyo, Japan
[20] now at Kobe University, Japan
[21] supported by DESY, Germany
[22] partially supported by Russian Foundation for Basic Research grant No. 05-02-39028-NSFC-a
[23] STFC Advanced Fellow
[24] nee Korcsak-Gorzo
[25] This material was based on work supported by the National Science Foundation, while working at the Foundation.
[26] also at Max Planck Institute, Munich, Germany, Alexander von Humboldt Research Award
[27] now at KEK, Tsukuba, Japan
[28] now at Nagoya University, Japan
[29] member of Department of Radiological Science, Tokyo Metropolitan University, Japan
[30] now at SunMelx Co. Ltd., Tokyo, Japan
[31] now at University of Bonn, Germany
[32] also at Hamburg University, Inst. of Exp. Physics, Alexander von Humboldt Research Award and partially supported by DESY, Hamburg, Germany
[33] also at Łódź University, Poland
[34] member of Łódź University, Poland
[35] now at Lund University, Lund, Sweden
† deceased

[a] supported by the Natural Sciences and Engineering Research Council of Canada (NSERC)

[b] supported by the German Federal Ministry for Education and Research (BMBF), under contract Nos. 05 HZ6PDA, 05 HZ6GUA, 05 HZ6VFA and 05 HZ4KHA

[c] supported in part by the MINERVA Gesellschaft für Forschung GmbH, the Israel Science Foundation (grant No. 293/02-11.2) and the US-Israel Binational Science Foundation

[d] supported by the Israel Science Foundation

[e] supported by the Italian National Institute for Nuclear Physics (INFN)

[f] supported by the Japanese Ministry of Education, Culture, Sports, Science and Technology (MEXT) and its grants for Scientific Research

[g] supported by the Korean Ministry of Education and Korea Science and Engineering Foundation

[h] supported by the Netherlands Foundation for Research on Matter (FOM)

[i] supported by the Polish State Committee for Scientific Research, project No. DESY/256/2006 - 154/DES/2006/03

[j] partially supported by the German Federal Ministry for Education and Research (BMBF)

[k] supported by RF Presidential grant N 1456.2008.2 for the leading scientific schools and by the Russian Ministry of Education and Science through its grant for Scientific Research on High Energy Physics

[l] supported by the Spanish Ministry of Education and Science through funds provided by CICYT

[m] supported by the Science and Technology Facilities Council, UK

[n] supported by the US Department of Energy

[o] supported by the US National Science Foundation. Any opinion, findings and conclusions or recommendations expressed in this material are those of the authors and do not necessarily reflect the views of the National Science Foundation.

[p] supported by the Polish Ministry of Science and Higher Education as a scientific project (2009-2010)

[q] supported by FNRS and its associated funds (IISN and FRIA) and by an Inter-University Attraction Poles Programme subsidised by the Belgian Federal Science Policy Office

[r] supported by an FRGS grant from the Malaysian government

# 1 Introduction

In the HERA photoproduction regime, where the virtuality of the exchanged photon is small, the production of inelastic $J/\psi$ mesons is dominated by boson-gluon fusion: a photon emitted from the incoming lepton interacts with a gluon coming from the proton to produce a $c\bar{c}$ pair which subsequently forms a $J/\psi$ meson. Production of $J/\psi$ through boson-gluon fusion can be calculated using perturbative Quantum Chromodynamics (pQCD) in the colour-singlet (CS), in the non-relativistic QCD (NRQCD) [1, 2] and in the $k_T$-factorisation frameworks [3, 4].

In the CS approach, only the colourless $c\bar{c}$ pair produced in the hard subprocess can lead to a physical $J/\psi$ state. In the NRQCD approach, a $c\bar{c}$ pair emerging from the hard process in a colour-octet (CO) state can also evolve into a $J/\psi$ state with a probability proportional to universal long-distance matrix elements (LDME) that are obtained from experiment. In the $k_T$-factorisation approach, the effects of non-zero incoming parton transverse momentum are taken into account. Cross sections are then calculated in the CS approach as a convolution of unintegrated (transverse-momentum dependent) parton densities and leading-order (LO) off-shell matrix elements.

At HERA, measurements of inelastic $J/\psi$ differential cross sections [5,6] are reproduced by a next-to-leading-order (NLO) QCD calculation [7,8] performed in the CS framework. The measurements are also reasonably well described by LO CS plus CO calculations [9–11], with LDME as determined in a LO analysis of hadroproduction and $B$-decay data [12–15].

The polar and azimuthal distributions of the $J/\psi$ decay leptons in the $J/\psi$ rest frame may be used to distinguish between CS and CO models. These helicity distributions are expected to be different as a function of the $J/\psi$ transverse momentum, $p_T$, and inelasticity, the fraction of the incident photon energy carried by the $J/\psi$ in the proton rest frame, $z$ [16].

Helicity-distribution measurements have already been performed by the ZEUS [5] and H1 [6] collaborations. In the final study presented here, $J/\psi$ mesons were identified using the decay mode $J/\psi \to \mu^+\mu^-$ and were measured in the range $50 < W < 180$ GeV, where $W$ is the photon-proton centre-of-mass energy. The data sample under study includes the data used in the previously published ZEUS analysis [5] and corresponds to an increase in statistics of a factor of 12.

## 2 Experimental set-up

The analysis presented here is based on data collected by the ZEUS detector at HERA in the period 1996–2007. In 1998–2007 (1996–1997), HERA provided electron[1] beams of energy $E_e = 27.5$ GeV and proton beams of energy $E_p = 920$ (820) GeV, resulting in a centre-of-mass energy of $\sqrt{s} = 318$ (300) GeV, corresponding to an integrated luminosity of $430 \pm 11$ ($38 \pm 0.6$) pb$^{-1}$.

A detailed description of the ZEUS detector can be found elsewhere [17, 18]. A brief outline of the components that are most relevant for this analysis is given below. Charged particles were tracked in the central tracking detector (CTD) [19], which operated in a magnetic field of 1.43 T provided by a thin superconducting coil. Before the 2003–2007 running period, the ZEUS tracking system was upgraded with a silicon microvertex detector (MVD) [20]. The high-resolution uranium–scintillator calorimeter (CAL) [21] consisted of three parts: the forward (FCAL), the barrel (BCAL) and the rear (RCAL) calorimeters[2].

Muons were identified by tracks in the barrel and rear muon chambers (BMUON and RMUON) [22]. The muon chambers were placed inside and outside the magnetised iron yoke surrounding the CAL. The barrel and rear inner muon chambers (BMUI and RMUI) covered the polar-angle regions $34^\circ < \theta < 135^\circ$ and $135^\circ < \theta < 171^\circ$, respectively. The luminosity was measured using the Bethe–Heitler reaction $ep \to e\gamma p$ with the luminosity detector which consisted of a lead–scintillator calorimeter [23] and, after 2002, an additional magnetic spectrometer [24] system.

## 3 Event selection

Inelastic events are often selected using the inelasticity, $z$. In this analysis, however, the events were selected using the transverse momentum, $p_T$, of the $J/\psi$ and additional activity in the detector. This kind of selection permits direct comparisons with the different theoretical predictions [16].

The online and offline selections as well as the reconstruction of the kinematic variables closely follow a previous analysis [5].

[1] Here and in the following, the term "electron" denotes generically both the electron ($e^-$) and the positron ($e^+$).

[2] The ZEUS coordinate system is a right-handed Cartesian system, with the $Z$ axis pointing in the proton beam direction, referred to as the "forward direction", and the $X$ axis pointing towards the centre of HERA. The coordinate origin is at the nominal interaction point. The polar angle, $\theta$, is measured with respect to the proton beam direction. The pseudorapidity is defined as $\eta = -\ln(\tan\frac{\theta}{2})$.

Online, the BMUI and RMUI chambers were used to tag muons by matching segments in the muon chambers with tracks in the CTD/MVD, as well as with energy deposits in the CAL consistent with the passage of a minimum-ionising particle (m.i.p.).

Offline, an event was accepted if it had two tracks forming a $J/\psi$ candidate. One track had to be identified in the inner muon chambers and matched to a m.i.p. cluster in the CAL. It was required to have a momentum greater than 1.8 GeV if it was in the rear region, or a transverse momentum greater than 1.4 GeV if in the barrel region. The other track had to be matched to a m.i.p. cluster in the CAL and was required to have a transverse momentum greater than 0.9 GeV. Both tracks were restricted to the pseudorapidity region $|\eta| < 1.75$. To reject cosmic rays, events in which the angle between the two muon tracks was larger than 174° were removed.

The $p_T$ of the $J/\psi$ candidate was required to be larger than 1 GeV. In addition, events were required to have an energy deposit larger than 1 GeV in a cone of 35° around the forward direction (excluding possible calorimeter deposits due to the decay muons). According to Monte Carlo (MC) simulations, these requirements completely reject exclusively produced $J/\psi$ mesons ($ep \to epJ/\psi$) as well as proton-diffractive events ($ep \to eYJ/\psi$) in which the mass of the proton dissociative state, $M_Y$, is below 4.4 GeV. To further reduce diffractive background, events were also required to have at least one additional track with a transverse momentum larger than 0.125 GeV and pseudorapidity $|\eta| < 1.75$.

# 4 Kinematic variables and signal extraction

The photon-proton centre-of-mass energy, $W$, is:

$$W^2 = (P + q)^2, \tag{1}$$

where $P$ and $q$ are the four–momenta of the incoming proton and exchanged photon, respectively. It was calculated using:

$$W^2 = 2E_p(E - p_Z) \tag{2}$$

where $(E - p_Z)$ is summed over all final-state energy-flow objects [25] (EFOs) which combine the information from calorimetry and tracking.

The inelasticity $z = \frac{P \cdot p_{J/\psi}}{P \cdot q}$ was determined as:

$$z = \frac{(E - p_Z)_{J/\psi}}{(E - p_Z)}, \tag{3}$$

where $p_{J/\psi}$ is the four-momentum of the $J/\psi$ and $(E - p_Z)_{J/\psi}$ was calculated using the tracks forming the $J/\psi$.

The kinematic region considered was $50 < W < 180$ GeV where the acceptance was always above 10%. A requirement of $E - p_Z < 20$ GeV restricted the virtuality of the exchanged photon $Q^2 = -q^2 \lesssim 1$ GeV$^2$, with a median of $\approx 10^{-4}$ GeV$^2$. The elimination of deep inelastic scattering events was independently confirmed by searching for scattered electrons in the CAL [26]; none was found.

The invariant-mass spectrum of the $J/\psi$ candidates with $p_T > 1$ GeV and $z > 0.1$ is shown in Fig. 1. Both the $J/\psi$ and $\psi'$ peaks are visible. The background was estimated by fitting the product of a second-order polynomial and an exponential to the region outside the invariant-mass window, 2.85–3.3 GeV. The number of $J/\psi$ events was obtained by subtracting the number of background events estimated from the fit procedure from the total number of events inside the invariant-mass window; $12310 \pm 140$ $J/\psi$ events were found. As the signal to background ratio is large, the extracted number of $J/\psi$ events has little sensitivity to the analytical form of the function used for the background fit.

# 5 Monte Carlo and background evaluation

The inelastic production of $J/\psi$ mesons was simulated using the HERWIG 5.8 [27] MC generator, which generates events according to the LO diagrams of the boson-gluon-fusion process, $\gamma g \to J/\psi g$, as calculated in the framework of the CS model. This process is called a direct photon process, because the incoming photon couples to the $c$ quark directly. The HERWIG MC sample was reweighted in $p_T$, $z$ and $W$ in order to give the best description of the data.

There are other sources of $J/\psi$ mesons which were classified as background in the present analysis and were estimated either from MC models or previous measurements. Although the relative rate of each process is given below, the helicity distributions of these $J/\psi$ sources are poorly known, so the contributions were not subtracted.

Diffractive production of $J/\psi$ mesons with proton dissociation was simulated with the EPSOFT [28] MC generator, which was tuned to describe such processes at HERA [29]. This background is suppressed by the requirement on the tracks and by the cut on the minimum $p_T$ of the $J/\psi$. The overall contribution of this background is 6%; it is largest in the lowest $p_T$ bin ($1 \le p_T \le 1.4$ GeV), where it is 7.5%, and in the highest $z$ bin ($0.9 \le z \le 1$), where it is 66%.

The production of $J/\psi$ mesons originating from $B$-meson decays was simulated using the PYTHIA 6.2 MC generator [30]. The beauty-quark mass was set to 4.75 GeV and the $B$ to $J/\psi$ branching ratio was set to the PDG value [31]. According to the MC, 1.6% of the observed $J/\psi$ events were from $B$-meson decays; the fraction is largest in the highest $p_T$

bin ($4.2 \leq p_T \leq 10$ GeV), where it is equal to 6.3%, and in the lowest $z$ bin ($0.1 \leq z \leq 0.4$), where it is 8.4%.

The background from $\psi^{'}$ to $J/\psi$ decays is expected to be around 15%, as obtained using the direct measurement of the $\psi^{'}$ to $J/\psi$ cross section ratio [5] and the branching ratio of the $\psi'$ to $J/\psi$.

All generated events were passed through a full simulation of the ZEUS detector based on GEANT 3 [32]. They were then subjected to the same trigger requirements and processed by the same reconstruction program as the data.

# 6 Reconstruction of the helicity parameters

The helicity analysis was performed in the so-called "target frame" [16], i.e. the $J/\psi$ rest frame with the axes $Z' = -Z$ and $Y'$ along the vector $\vec{q'} \times (-\vec{P'})$, where $\vec{q'}$ and $\vec{P'}$ are the three-vectors associated with the exchanged photon and incoming proton. The polar and azimuthal angles of the $\mu^+$ in this frame are denoted $\theta^\star$ and $\phi^\star$.

The differential cross sections in $\theta^\star$ and $\phi^\star$ can be parametrised as [16]:

$$\frac{d\sigma}{d\cos\theta^\star} \propto 1 + \lambda \cos^2\theta^\star, \tag{4}$$

and

$$\frac{d\sigma}{d\phi^\star} \propto 1 + \frac{\lambda}{3} + \frac{\nu}{3}\cos 2\phi^\star, \tag{5}$$

where $\lambda$ and $\nu$, the polar and azimuthal angular parameters, are functions of $p_T$ and $z$. The predictions for $\lambda$ and $\nu$ depend on the production mechanism. The value $\lambda = +1$ corresponds to $J/\psi$ mesons fully transversally polarised, while $\lambda = -1$ corresponds to $J/\psi$ mesons fully longitudinally polarised.

The $\lambda$ and $\nu$ parameters were determined in bins of $z$ and $p_T$, each time integrating over the other variable. As a function of $p_T$, the integration range for $z$ was set to $0.4 < z < 1$, thereby avoiding the region $0.1 < z < 0.4$ where the ratio of signal to combinatorial background is rather poor (0.52). The integration range in $p_T$ started at $p_T = 1$ GeV.

In the estimation of the parameters $\lambda$ and $\nu$, the helicity distributions of the background events present under the $J/\psi$ peak were added to the MC distributions. The shape of the background helicity distributions was taken from the side bands, while the number of background events was taken from the fits described in Section 4.

The HERWIG MC generator-level distributions $dN/d\cos\theta^\star$ ($dN/d\phi^\star$) were re-weighted according to Eq. 4 (5) within a search grid of $\lambda$ ($\nu$) values. For each re-weighted distribution, the value of $\chi^2$ was calculated from a comparison to the data. The $\lambda$ ($\nu$) value

providing the minimum $\chi^2$, $\chi^2_{\rm min}$, was taken as the central value. The parameter values with $\chi^2 = \chi^2_{\rm min} + 1$ were used to calculate the statistical uncertainties. The $\chi^2_{\rm min}$ per degree of freedom were typically around one. Equation 4 was first used to extract $\lambda$, and then $\lambda$ was inserted into Eq. 5 to extract $\nu$, see Tables 1 and 2.

# 7 Systematic uncertainties

The following sources of systematic uncertainties were investigated (their effects are given in parentheses):

- muon chamber efficiencies: the BMUI and RMUI muon chamber efficiencies were extracted from the data using muon pairs coming from elastic $J/\psi$ events and from the process $\gamma\gamma \to \mu^+\mu^-$. These efficiencies are known up to an uncertainty of about $\pm 5\%$ ($< 5\%$ of the statistical error);
- analysis cuts: this class comprises the systematic uncertainties due to the uncertainties in the measurement of momentum, transverse momentum and pseudorapidity of the muon decay tracks. Each cut was varied within a range determined by the resolution in the appropriate variable ($< 5\%$ of the statistical error);
- CAL energy scale: the CAL energies were varied by $\pm 5\%$ in the simulation, in accordance with the uncertainty in the CAL energy scale (on average 10% of the statistical error);
- hadronic energy resolution: the $W$ and $z$ resolutions are dominated by the hadronic energy resolution affecting the quantity $(E - p_Z)$. The $(E - p_Z)$ resolution in the MC was smeared event by event by $\pm 20\%$ (on average 10% of the statistical error);
- $p_T$, $W$ and $z$ spectra: the $p_T$, $W$ and $z$ spectra of the $J/\psi$ mesons in the HERWIG MC simulation were varied within ranges allowed by the comparison between data and simulation (on average 15% of the statistical error);
- additional track requirement: the kinematic cuts for the additional track requirement were tightened and loosened in both data and MC (on average 15% of the statistical error);
- influence of diffractive contamination at high $z$ on the $\lambda$ and $\nu$ extractions as a function of $p_T$: $\lambda$ and $\nu$ were extracted changing the $z$ integration range from $0.4 < z < 1$ to $0.4 < z < 0.9$ (on average 25% of the statistical error);
- angular coverage in $\theta^\star$: $\cos\theta^\star$ was restricted to the range $-0.8 < \cos\theta^\star < 0.8$ in order to avoid low-acceptance regions (on average 30% of the statistical error);

- invariant-mass window: the $J/\psi$ invariant mass window was enlarged by 50 MeV and tightened by 100 MeV (on average 30% of the statistical error).

All of the above individual sources of systematic uncertainty were added in quadrature. No systematic uncertainties are quoted for $J/\psi$ coming from $B$-meson decays and $J/\psi$ coming from $\psi'$ decays. The uncertainties on the integrated-luminosity determination and on the $J/\psi \to \mu^+\mu^-$ branching ratio, which would result in an overall shift of a cross section measurement, do not contribute to the measurement of the helicity parameters.

# 8 Results

The values of the parameter $\lambda$ are shown as a function of $p_T$ and $z$ in Fig. 2a) and b), respectively; the values of the parameter $\nu$ are displayed in Fig. 3a) and b). All the values are also listed in Tables 1 and 2. The data indicate that the parameter $\lambda$ depends, if at all, only weakly on $p_T$ and rises slowly with $z$. The parameter $\nu$ does not seem to depend on $p_T$, while it seems to increase at low and high $z$.

The data are compared to various theoretical predictions for photoproduction at $Q^2 = 0$. These predictions do not consider the polarisation due to $J/\psi$ coming from $\psi'$ decays, $B$-meson decays and from diffractive processes. The curves identified by the label LO CS show the LO prediction in the CS framework including both direct and resolved[3] processes. The two lines identified by the label LO + $k_T$ (JB) and LO + $k_T$ (dGRV), represent the predictions of a $k_T$-factorisation model [33] using two different unintegrated gluon distributions and including only direct processes. The band identified by the label NLO CS represents the predictions of a NLO calculation [34,35] including only direct processes. The width of the band gives the uncertainties of the calculation due to variations of the renormalisation and factorisation scales. It stops at $z = 0.9$ because no reliable predictions can be obtained near $z = 1$ for this fixed-order calculation. The band, identified by the label LO CS+CO, shows the LO prediction [16] including both CS and CO terms, including both direct and resolved processes. The width of the band results from the uncertainties in the values of the long-distance matrix elements. In Fig. 2a) and 3a), with $z$ integrated up to $z = 1$, the LO CS+CO cross section is CO dominated.

None of the models provides predictions for both $\lambda$ and $\nu$ that agree well with the data everywhere in $z$ and $p_T$. For $\lambda$ as a function of $p_T$, all the models roughly describe the data, with the NLO CS prediction providing the poorest description. For high values of $p_T$, the polarisation in the data remains small, while LO CS predicts a progressive

[3] In these resolved processes, the incoming photon does not couple to the $c$ quark directly, but via its hadronic component. They are expected to contribute mainly to the region of $z < 0.4$.

increase and NLO CS and LO $k_T$ a progressive decrease. The LO CS + CO prediction remains flat, with a small and positive value of $\lambda$. For $\lambda$ as a function of $z$, all theoretical predictions are in rough agreement with the data. The $p_T$ and $z$ dependencies of $\nu$ are not described by the LO CS predictions, while the other models provide better descriptions of the data.

The NLO CS calculation for $p_T > 1$ GeV suffers from large scale uncertainties connected to the presence of negative values of the diagonal components of the spin density matrix at $p_T \lesssim 1$ GeV [34, 35]. In order to avoid this problem, measurements and calculations were repeated increasing the $p_T$ cut first to 2 GeV and then to 3 GeV. In Fig. 4a) and b) the $\lambda$ and $\nu$ parameters, respectively, are shown as a function of $z$ for $p_T > 2$ GeV, while in Fig. 4c) and d) the same parameters are displayed for $p_T > 3$ GeV. All the values are listed in Table 3. The NLO CS calculation [35], also shown in these figures, has now smaller uncertainties, but the agreement with the data is only satisfactory for the $\nu$ parameter. Sizeable discrepancies remain for the $\lambda$ parameter both for $p_T > 2$ GeV and $p_T > 3$ GeV.

# 9 Conclusions

The $J/\psi$ helicity distributions in the inelastic photoproduction regime have been measured using a luminosity of 468 pb$^{-1}$. The $J/\psi$ helicity parameters $\lambda$ and $\nu$ were extracted in the target frame as a function of the transverse momentum and of the inelasticity of the $J/\psi$. The results were compared to LO QCD predictions in the colour-singlet, colour-singlet plus colour-octet and $k_T$ factorisation frameworks. A recent NLO QCD prediction in the colour-singlet framework was also considered. Even though the experimental and theoretical uncertainties are large, none of the predictions can describe all aspects of the data.

# Acknowledgments

We appreciate the contributions to the construction and maintenance of the ZEUS detector of many people who are not listed as authors. The HERA machine group and the DESY computing staff are especially acknowledged for their success in providing excellent operation of the collider and the data analysis environment. We thank the DESY directorate for their strong support and encouragement. It is a pleasure to thank P. Artoisonet, S.M. Baranov, M. Krämer and F. Maltoni for helpful discussions and for providing their predictions.

# References


[1] M. Krämer, Prog. Part. Nucl. Phys. **47**, 141 (2001).

[2] N. Brambilla et al., CERN Yellow Report, CERN-2005-005, Geneva.

[3] S.P. Baranov, Phys. Lett. **B 428**, 377 (1998).

[4] A.V. Lipatov and N.P. Zotov, Eur. Phys. J. **C 27**, 87 (2003).

[5] ZEUS Coll., S. Chekanov et al., Eur. Phys. J. **C 27**, 173 (2003).

[6] H1 Coll., C. Adloff et al., Eur. Phys. J. **C 25**, 25 (2002).

[7] M. Krämer et al., Phys. Lett. **B 348**, 657 (1995).

[8] M. Krämer, Nucl. Phys. **B 459**, 3 (1996).

[9] M. Cacciari and M. Krämer, Phys. Rev. Lett. **76**, 4128 (1996).

[10] B.A. Kniehl and G. Kramer, Eur. Phys. J. **C 6**, 493 (1999).

[11] M. Beneke, G.A. Schuler and S. Wolf, Phys. Rev. **D 62**, 34004 (2000).

[12] M. Beneke and M. Krämer, Phys. Rev. **D 55**, 5269 (1997).

[13] M. Beneke and I.Z. Rothstein, Phys. Rev. **D 54**, 2005 (1996).

[14] P. Ko, J. Lee and H.S. Song, Phys. Rev. **D 54**, 4312 (1996).

[15] S. Fleming et al., Phys. Rev. **D 55**, 4098 (1997).

[16] M. Beneke, M. Krämer and M. Vänttinen, Phys. Rev. **D 57**, 4258 (1998).

[17] ZEUS Coll., M. Derrick et al., Phys. Lett. **B 293**, 465 (1992).

[18] ZEUS Coll., U. Holm (ed.), *The ZEUS Detector*. Status Report (unpublished), DESY (1993), available on `http://www-zeus.desy.de/bluebook/bluebook.html`.

[19] N. Harnew et al., Nucl. Inst. Meth. **A 279**, 290 (1989);
B. Foster et al., Nucl. Phys. Proc. Suppl. **B 32**, 181 (1993);
B. Foster et al., Nucl. Inst. Meth. **A 338**, 254 (1994).

[20] A. Polini et al., Nucl. Inst. Meth. **A 581**, 31 (2007).

[21] M. Derrick et al., Nucl. Inst. Meth. **A 309**, 77 (1991);
A. Andresen et al., Nucl. Inst. Meth. **A 309**, 101 (1991);
A. Caldwell et al., Nucl. Inst. Meth. **A 321**, 356 (1992);
A. Bernstein et al., Nucl. Inst. Meth. **A 336**, 23 (1993).

[22] G. Abbiendi et al., Nucl. Inst. Meth. **A 333**, 342 (1993).

[23] J. Andruszków et al., Preprint DESY-92-066, DESY, 1992;
ZEUS Coll., M. Derrick et al., Z. Phys. **C 63**, 391 (1994);
J. Andruszków et al., Acta Phys. Pol. **B 32**, 2025 (2001).

[24] M. Helbich et al., Nucl. Inst. Meth. **A 565**, 572 (2006).

[25] ZEUS Coll., J. Breitweg et al., Eur. Phys. J. **C 1**, 81 (1998);
G.M. Briskin, Ph.D. Thesis, Tel Aviv University, Report DESY-THESIS 1998-036, 1998.

[26] H. Abramowicz, A. Caldwell and R. Sinkus, Nucl. Inst. Meth. **A 365**, 508 (1995).

[27] G. Marchesini et al., Comp. Phys. Comm. **67**, 465 (1992).

[28] M. Kasprzak, Ph.D. Thesis, Warsaw University, Warsaw, Poland, Report DESY F35D-96-16, DESY, 1996.

[29] L. Adamczyk, Ph.D. Thesis, University of Mining and Metallurgy, Cracow, Poland, Report DESY-THESIS-1999-045, DESY, 1999.

[30] T. Sjöstrand et al., Comp. Phys. Comm. **135**, 238 (2001);
E. Norrbin and T. Sjöstrand, Eur. Phys. J. **C 17**, 137 (2000);
T. Sjöstrand, L. Lönnblad, and S. Mrenna, Preprint hep-ph/0108264, 2001.

[31] Particle Data Group, C. Amsler et al., Phys. Lett. **B 667**, 1 (2008).

[32] R. Brun et al., GEANT3, Technical Report CERN-DD/EE/84-1, CERN, 1987.

[33] S.P. Baranov, JETP **88**, 471 (2008).

[34] P. Artoisenet et al., Preprint arXiv:0901.4352, 2009.

[35] P. Artoisenet, private communication, 2009.

| $p_T$ range (GeV) | $\langle p_T \rangle$ (GeV) | $\lambda$ | $\nu$ |
|---|---|---|---|
| 1.0 – 1.4 | 1.2 | $0.16^{+0.15\ +0.10}_{-0.16\ -0.04}$ | $0.26^{+0.10\ +0.05}_{-0.10\ -0.08}$ |
| 1.4 – 1.9 | 1.6 | $0.38^{+0.17\ +0.10}_{-0.17\ -0.10}$ | $-0.12^{+0.12\ +0.07}_{-0.14\ -0.01}$ |
| 1.9 – 2.4 | 2.1 | $-0.15^{+0.17\ +0.20}_{-0.17\ -0.08}$ | $-0.33^{+0.21\ +0.12}_{-0.24\ -0.16}$ |
| 2.4 – 3.4 | 2.8 | $0.21^{+0.17\ +0.26}_{-0.16\ -0.05}$ | $-0.09^{+0.19\ +0.13}_{-0.20\ -0.13}$ |
| 3.4 – 4.2 | 3.7 | $0.34^{+0.32\ +0.16}_{-0.28\ -0.17}$ | $0.21^{+0.26\ +0.10}_{-0.28\ -0.03}$ |
| 4.2 – 10. | 5.2 | $0.31^{+0.33\ +0.21}_{-0.31\ -0.19}$ | $-0.50^{+0.27\ +0.11}_{-0.28\ -0.07}$ |

**Table 1:** *$J/\psi$ helicity parameters $\lambda$ and $\nu$ as a function of $p_T$ measured in the target frame for $50 < W < 180$ GeV, $0.4 < z < 1$ and $p_T > 1$ GeV. The first uncertainty is statistical and the second is systematic.*

| $z$ range | $\langle z \rangle$ | $\lambda$ | $\nu$ |
|---|---|---|---|
| 0.10 – 0.40 | 0.27 | $0.27^{+0.43\ +0.13}_{-0.40\ -0.14}$ | $0.99^{+0.24\ +0.14}_{-0.27\ -0.40}$ |
| 0.40 – 0.55 | 0.48 | $-0.22^{+0.19\ +0.18}_{-0.18\ -0.06}$ | $-0.01^{+0.17\ +0.08}_{-0.18\ -0.03}$ |
| 0.55 – 0.70 | 0.61 | $0.16^{+0.12\ +0.10}_{-0.13\ -0.04}$ | $-0.05^{+0.10\ +0.05}_{-0.11\ -0.02}$ |
| 0.70 – 0.80 | 0.75 | $0.39^{+0.15\ +0.04}_{-0.15\ -0.13}$ | $-0.07^{+0.11\ +0.04}_{-0.13\ -0.07}$ |
| 0.80 – 0.90 | 0.85 | $0.30^{+0.17\ +0.15}_{-0.17\ -0.05}$ | $0.04^{+0.14\ +0.08}_{-0.15\ -0.08}$ |
| 0.90 – 1.0 | 0.95 | $0.49^{+0.39\ +0.15}_{-0.34\ -0.08}$ | $0.54^{+0.26\ +0.16}_{-0.28\ -0.08}$ |

**Table 2:** *$J/\psi$ helicity parameters $\lambda$ and $\nu$ as a function of $z$ measured in the target frame for $50 < W < 180$ GeV, $0.1 < z < 1$ and $p_T > 1$ GeV. The first uncertainty is statistical and the second is systematic.*

| $p_T$ range (GeV) | $z$ range | $\langle z \rangle$ | $\lambda$ | $\nu$ |
|---|---|---|---|---|
| $p_T > 2$ | 0.10 – 0.55 | 0.37 | $0.35^{+0.34\ +0.04}_{-0.31\ -0.41}$ | $-0.37^{+0.35\ +0.08}_{-0.39\ -0.09}$ |
| | 0.55 – 0.70 | 0.61 | $0.05^{+0.18\ +0.20}_{-0.17\ -0.06}$ | $-0.10^{+0.19\ +0.08}_{-0.20\ -0.05}$ |
| | 0.70 – 0.80 | 0.75 | $0.34^{+0.22\ +0.04}_{-0.22\ -0.17}$ | $-0.05^{+0.21\ +0.06}_{-0.23\ -0.25}$ |
| | 0.80 – 0.90 | 0.85 | $0.12^{+0.24\ +0.29}_{-0.23\ -0.08}$ | $-0.39^{+0.26\ +0.22}_{-0.27\ -0.01}$ |
| $p_T > 3$ | 0.10 – 0.55 | 0.38 | $0.80^{+0.53\ +0.11}_{-0.45\ -0.43}$ | $0.07^{+0.40\ +0.07}_{-0.44\ -0.04}$ |
| | 0.55 – 0.70 | 0.62 | $0.26^{+0.31\ +0.23}_{-0.28\ -0.06}$ | $-0.26^{+0.27\ +0.20}_{-0.28\ -0.06}$ |
| | 0.70 – 0.90 | 0.79 | $0.09^{+0.25\ +0.27}_{-0.23\ -0.12}$ | $-0.35^{+0.27\ +0.09}_{-0.28\ -0.07}$ |

**Table 3:** *$J/\psi$ helicity parameters $\lambda$ and $\nu$ as a function of $z$ measured in the target frame for $50 < W < 180$ GeV, $0.1 < z < 1$ and for $p_T > 2$ and $p_T > 3$ GeV. The first uncertainty is statistical and the second is systematic.*

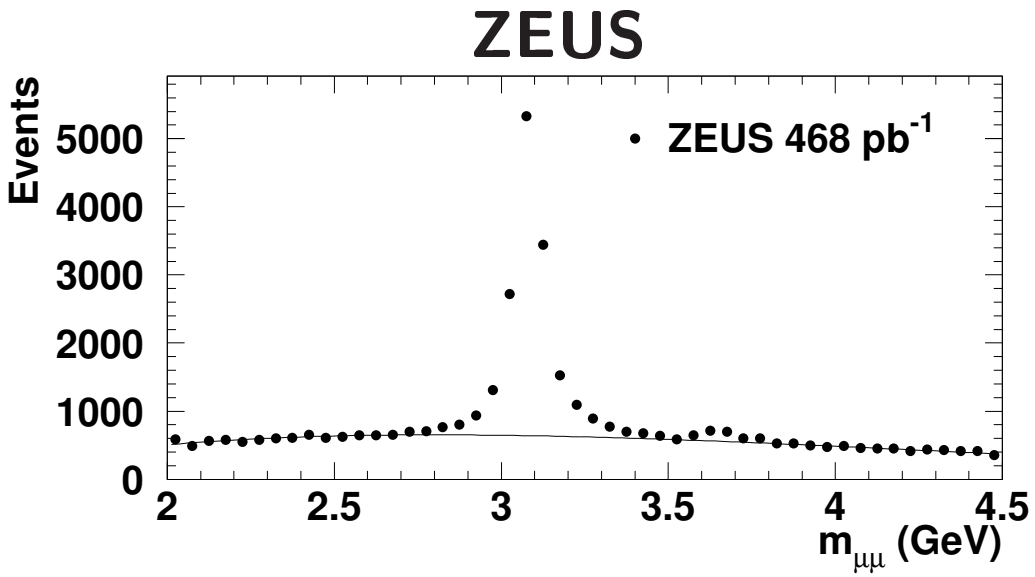


**Figure 1:** *Dimuon invariant mass, $m_{\mu\mu}$, spectrum in the phase-space region $50 < W < 180$ GeV, $z > 0.1$ and $p_T > 1$ GeV. The continuous line represents the fitted background.*

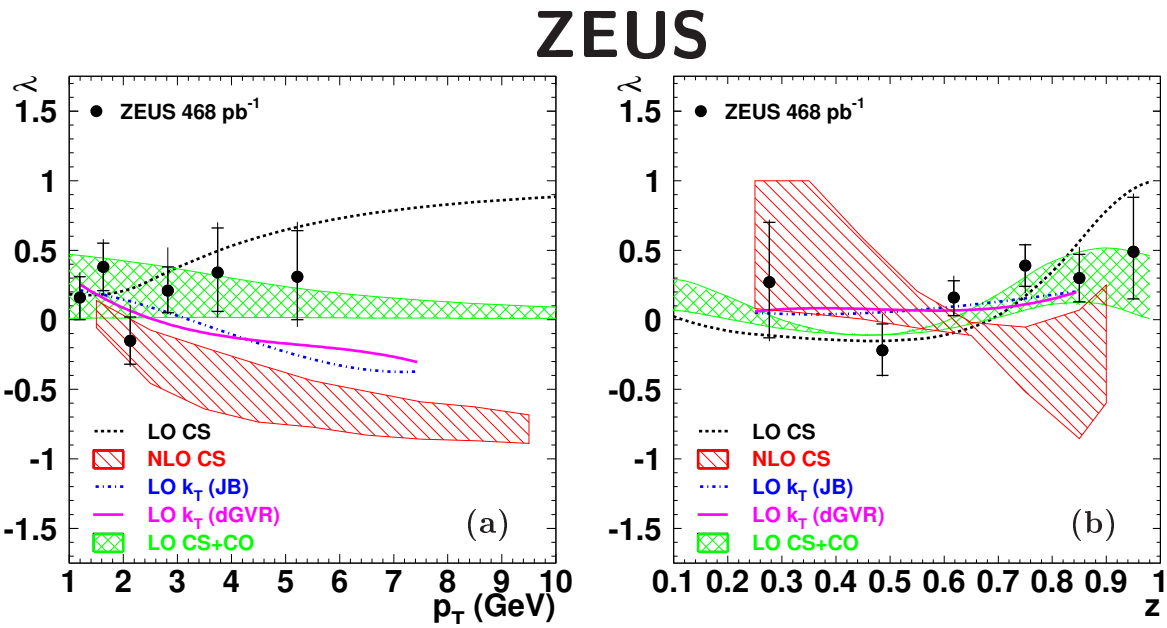


**Figure 2:** *The helicity parameter $\lambda$, measured in the target frame, as a function of (a) $p_T$, and (b) $z$. The measurement is performed in the kinematic range $50 < W < 180$ GeV, $0.1 < z < 1$ and $p_T > 1$ GeV. The measurement as a function of $p_T$ is restricted to the kinematic range $0.4 < z < 1$. The inner (outer) error bars correspond to the statistical (total) uncertainty. The theoretical curves are described in the text.*

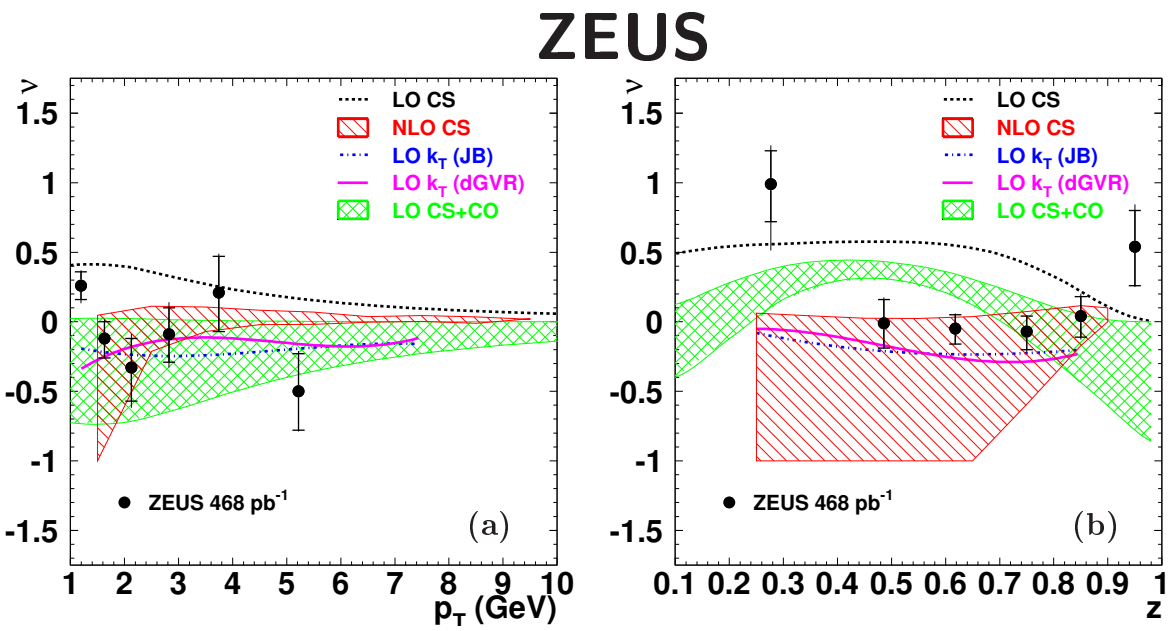


**Figure 3:** *The helicity parameter $\nu$, measured in the target frame, as a function of (a) $p_T$, and (b) $z$. The measurement is performed in the kinematic range $50 < W < 180$ GeV, $0.1 < z < 1$ and $p_T > 1$ GeV. The measurement as a function of $p_T$ is restricted to the kinematic range $0.4 < z < 1$. The inner (outer) error bars correspond to the statistical (total) uncertainty. The theoretical curves are described in the text.*

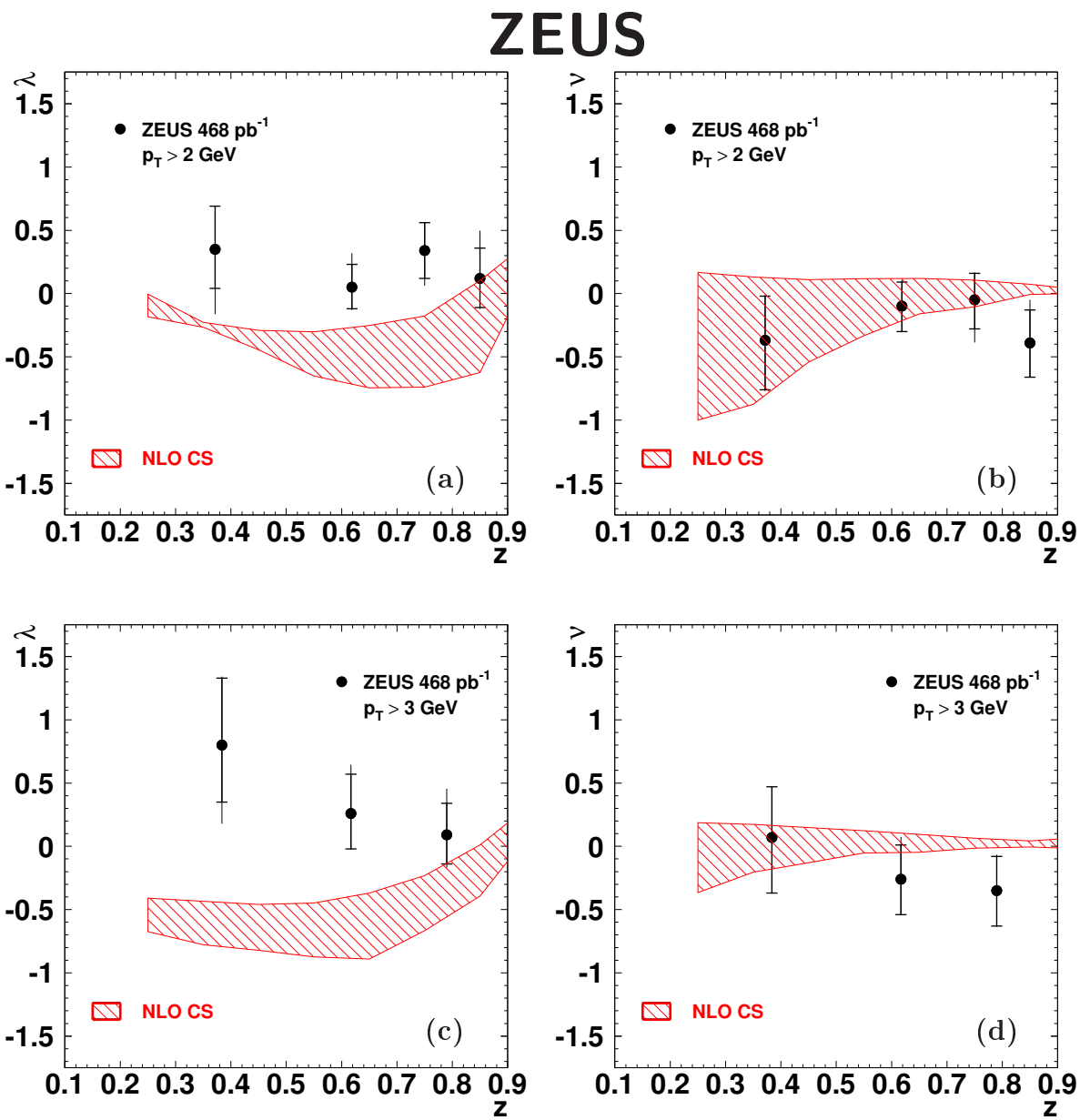


**Figure 4:** *Distributions of the helicity parameters (a), (c) $\lambda$ and (b), (d) $\nu$ as a function of $z$, measured in the target frame, for $50 < W < 180$ GeV, $0.1 < z < 0.9$ and (a), (b) $p_T > 2$ GeV and (c), (d) $p_T > 3$ GeV. The inner (outer) error bars correspond to the statistical (total) uncertainty. The theoretical bands are described in the text.*